

Poly (L-Lactic Acid)/Layered Silicate Nanocomposite: Fabrication, Characterization, and Properties

Vahik Krikorian and Darrin J. Pochan*

Department of Materials Science and Engineering and Delaware Biotechnology Institute,
University of Delaware, Newark, Delaware 19716

Received May 16, 2003. Revised Manuscript Received July 30, 2003

The possibility of making rigid polymer layered nanocomposites from biocompatible/biodegradable matrixes was explored. Three types of commercially available organophilic clay were employed to concurrently study the effects of organic modifier miscibility with the matrix and of the extent of clay modification on overall nanocomposite formation. The nanocomposites were fabricated via the exfoliation–adsorption technique with the matrix polymer poly (L-lactic acid), PLLA, a widely used, biodegradable, synthetic polyester. X-ray diffraction (XRD) data reveal that increasing the miscibility of the surfactant/polymer matrix increases the tendency of the system to exfoliate and randomly distribute the silicate layers. Transmission electron microscopy (TEM) data show that the ordering of silicate platelets is consistent with *d* spacings obtained from XRD. Because of the nanometer-range dispersion of silicate layers, all the nanocomposites retain their optical clarity. Mechanical properties of the fabricated nanocomposites were probed by dynamic mechanical analysis and show significant improvements in the storage modulus when compared to neat PLLA. The extent of crystallinity was observed to be inversely proportional to the extent of modified clay loading in the final composites.

Introduction

In the past decade, significant attention has been focused on biodegradable and biocompatible polymers, both from biomedical and ecological perspectives.¹ Generally, polymers that are produced from petrochemical products have low recovery/reproduction rates and are not easily degraded in the environment. The rapid growth of municipal waste volume drives efforts toward biodegradable polymers that can be used as renewable resources for polymer manufacturing and reduce plastic wastes. Polylactides are of significant interest in medical applications such as wound closure, surgical implants,² resorbable sutures,³ tissue culture,⁴ and controlled release systems.^{5–7} These are predominantly poly(ϵ -caprolactone) (PCL), poly(lactic acid) (PLA), and poly(glycolic acid) PGA, among which PLA has attracted the most attention due to its renewable resources,⁸ biodegradation, biocompatibility, superior thermal/mechanical properties, and the transparency of the processed materials.⁹ Biomedical use of PLA originated in the

early 1960s and has since become widely used in the medical field.¹⁰ PLA is commercially available in a variety of grades and has been approved by the U.S. Food and Drug Administration (FDA) for medical use.⁷

PLA is a linear, aliphatic, thermoplastic polyester, synthesized from renewable resources, and is readily biodegradable through hydrolytic¹¹ and enzymatic^{8,12} pathways. Upon in vivo degradation, PLA undergoes hydrolytic decomposition to lactic acid, a natural intermediate in carbohydrate metabolism.¹³ PLA can be produced by ring-opening polymerization of lactides or condensation polymerization of all stereoisomers of lactic acid monomers, pure D- or L-lactic acid or a racemic mixture of the two, which are produced by fermentation of corn, potato, sugar cane, and sugar beat, among other plant sources.¹⁴ A schematic view of the chemical structure of the pure L stereoisomer, or poly(L-Lactic acid) (PLLA), is illustrated in Figure 1. For the rest of the manuscript PLA refers to the racemic random copolymer of both stereoisomers of lactic acid, whereas PLLA refers specifically to the L stereoisomer homopolymer.

A wealth of investigations has been performed to enhance the impact resistance of PLA and compete with

* To whom correspondence should be addressd. E-mail: Pochan@udel.edu.

(1) Ikada, Y.; Tsuji, H. *Macromol. Rapid Commun.* **2000**, *21*, 117–132.

(2) Taylor, M. S.; Daniels, A. U.; Andriano, K. P.; Heller, J. *J. Appl. Biomater.* **1994**, *5*, 151–157.

(3) Jain, R. A. *Biomaterials* **2000**, *21*, 2475–2490.

(4) Mikos, A. G.; Lyman, M. D.; Freed, L. E.; Langer, R. *Biomaterials* **1994**, *15*, 55–58.

(5) Park, T. G.; Cohen, S.; Langer, R. *Macromolecules* **1992**, *25*, 116–122.

(6) Kamath, K. R.; Park, K. *Adv. Drug Delivery Rev.* **1993**, *11*, 59–84.

(7) Davis, S. S.; Illum, L.; Stolnik, S. *Curr. Opin. Colloid & Interface Sci.* **1996**, *1*, 660–666.

(8) Tsuji, H.; Ikada, Y. *J. Appl. Polym. Sci.* **1998**, *67*, 405–415.

(9) Urayama, H.; Kanamori, T.; Kimura, Y. *Macromol. Mater. Eng.* **2002**, *287*, 116–121.

(10) Edlund, U.; Albertsson, A. C. *Adv. Polym. Sci.* **2002**; Vol. 157, pp 67–112.

(11) Iwata, T.; Doi, Y. *Macromolecules* **1998**, *31*, 2461–2467.

(12) Sinclair, R. G. *J. Macromol. Sci., Pure Appl. Chem.* **1996**, *A33*, 585–597.

(13) Sawai, D.; Takahashi, K.; Imamura, T.; Nakamura, K.; Kanamoto, T.; Hyon, S. H. *J. Polym. Sci., Part B: Polym. Phys.* **2002**, *40*, 95–104.

(14) Kharas, G. B.; Sanchez-Riera, F.; Severson, D. K. *Plastics from Microbes*; Hanser Publishers: New York, 1994.

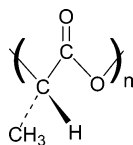


Figure 1. Chemical structure of poly(L-lactic acid) (PLLA).

low cost commodity polymers. These efforts have made use of biodegradable and nonbiodegradable plasticizers or by blending PLA with other polymers.¹⁵ From a biomedical point of view the mechanical properties of neat PLA might not be adequate for high-load-bearing applications¹⁶ which would necessitate the need for incorporation of reinforcements such as oriented PLA fibers, i.e., self-reinforced (SR) composites¹⁷ or hydroxyapatite (HA), a calcium phosphate similar to the inorganic content of bone.¹⁸

Polymer layered silicate nanocomposites (PLSN) have been the focus of academic and industrial attention in recent years because the final composites often exhibit a desired enhancement of physical and/or chemical properties relative to the neat polymer matrix, even at very low clay contents. Natural, synthetic, or organically modified clay, which in the pure state inherit a stacked structure of parallel silicate layers, is put in direct contact with the polymer matrix. Depending on the extent of compatibility between clay and the matrix, a microphase-separated conventional composite, intercalated, or exfoliated morphology can be obtained.¹⁹ There are several different nanocomposite fabrication techniques that vary from exfoliation-adsorption, including melt intercalation to in situ intercalative polymerization.²⁰ A diverse array of matrix polymers have been used in PLSN formation, ranging from biopolymer polypeptide-based nanocomposites²¹ to biocompatible polymers such as poly(ϵ -caprolactone)²² to commodity synthetic polymers such as nylon,²³ polystyrene,²⁴ poly(ethylene terephthalate),²⁵ polypropylene^{26,27} and polyurethanes,²⁸ just to name a few.

Recently, there have been several attempts to broaden the end-use properties of PLA by fabricating PLA/silicate-layered nanocomposites. Early work of Ogata et al.²⁹ ended up with micrometer-scale phase separation

of the organoclay filler with the PLA matrix without nanometer-range dispersion of silicate layers. In their investigation organically modified montmorillonite (MMT) was used to reinforce PLLA in composites produced via solution casting. Recently, Ray et al. and Maiti et al.^{30,31} have been able to produce intercalated nanocomposites with PLA by using organically modified clay and melt intercalation. They have shown the effects of clay particle size and clay cationic exchange capacity (CEC) on overall extent of intercalation. Lower CEC and smaller platelet size drove systems to higher extents of intercalation. However, highly ordered/stacked silicate layers were still observed and exfoliation was not achieved. Pluta et al.³² also investigated the feasibility of PLA nanocomposite formation by using organoclay and melt intercalation techniques. These studies observed both microphase separation of clay and polymer matrix and some intercalation of PLA into silicate layers but no clay exfoliation.

This publication describes our attempts to fabricate PLLA/organoclay nanocomposites via the exfoliation adsorption film casting technique. By varying the organic modifier used in clay modification we have studied the effect of modifier on the extent of silicate layer dispersion within the final PLLA/modified clay nanocomposite. By varying the hydrophobicity, and consequently the miscibility, of the organic modifier used in organoclay, a spectrum of intercalated toward fully exfoliated morphologies were obtained. To the best of our knowledge this is the first report of fully exfoliated/randomly distributed silicate layers within a PLLA matrix. The morphology of prepared nanocomposites was probed by X-ray diffraction (XRD) and supported by transmission electron microscopy (TEM). In addition, the effect of clay incorporation on the extent of PLLA crystallinity was studied by differential scanning calorimetry (DSC), and the effect of clay incorporation on the material property of viscoelastic storage modulus was measured by dynamic mechanical analysis (DMA).

Experimental Section

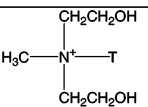
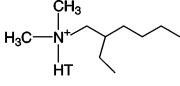
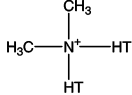
Materials. Poly(L-lactic acid) (PLLA) was purchased from Polysciences Inc. with a viscosity molecular weight of 325 000–460 000 g/mol as reported by the manufacturer. As-received PLLA was purified by dissolution in chloroform and subsequent precipitation with methanol. Refined polymer was then dried in vacuo for 2 days at 80 °C and kept in desiccation till later use. Three types of organically modified MMT, Cloisite 30B, 25A, and 15A, were purchased from Southern Clay Product Inc. and used as received. These organoclays are prepared by modification of natural montmorillonite clays with different quaternary ammonium salts. Extent of cationic exchange and the chemical structure of the specific organic modifier of each of the organoclays are listed in Table 1 according to the data provided by the supplier.

Nanocomposite Preparation. Nanocomposites were prepared by using the solution-intercalation film-casting technique. For each composition, 100 mg of PLLA was dissolved in 10 mL of dichloromethane. Clay dispersions (<0.1 wt %) were obtained by suspension of well-dried clay in a separate beaker of dichloromethane. Calculations for varying final

- (15) Martin, O.; Averous, L. *Polymer* **2001**, *42*, 6209–6219.
 (16) Bleach, N. C.; Nazhat, S. N.; Tanner, K. E.; Kellomaki, M.; Tormala, P. *Biomaterials* **2002**, *23*, 1579–1585.
 (17) Dauner, M.; Planck, H.; Caramaro, L.; Missirlis, Y.; Panagiotopoulos, E. *J. Mater. Sci.: Mater. Med.* **1998**, *9*, 173–179.
 (18) Shikunami, Y.; Okuno, M. *Biomaterials* **1999**, *20*, 859–877.
 (19) Giannelis, E. P. *Adv. Mater.* **1996**, *8*, 29.
 (20) Alexandre, M.; Dubois, P. *Mater. Sci. Eng., R* **2000**, *28*, 1–63.
 (21) Krikorian, V.; Kurian, M.; Galvin, M. E.; Nowak, A. P.; Deming, T. J.; Pochan, D. J. *J. Polym. Sci. Part B: Polym. Phys.* **2002**, *40*, 2579–2586.
 (22) Messersmith, P. B.; Giannelis, E. P. *Chem. Mater.* **1993**, *5*, 1064–1066.
 (23) Liu, L. M.; Qi, Z. N.; Zhu, X. G. *J. Appl. Polym. Sci.* **1999**, *71*, 1133–1138.
 (24) Weimer, M. W.; Chen, H.; Giannelis, E. P.; Sogah, D. Y. *J. Am. Chem. Soc.* **1999**, *121*, 1615–1616.
 (25) Ke, Y. C.; Long, C. F.; Qi, Z. N. *J. Appl. Polym. Sci.* **1999**, *71*, 1139–1146.
 (26) Hasegawa, N.; Kawasumi, M.; Kato, M.; Usuki, A.; Okada, A. *J. Appl. Polym. Sci.* **1998**, *67*, 87–92.
 (27) Kojima, Y.; Usuki, A.; Kawasumi, M.; Okada, A.; Kurauchi, T.; Kamigaito, O.; Kaji, K. *J. Polym. Sci. Part B: Polym. Phys.* **1995**, *33*, 1039–1045.
 (28) Chen, T. K.; Tien, Y. I.; Wei, K. H. *J. Polym. Sci. Part A: Polym. Chem.* **1999**, *37*, 2225–2233.
 (29) Ogata, N.; Jimenez, G.; Kawai, H.; Ogihara, T. *J. Polym. Sci. Part B: Polym. Phys.* **1997**, *35*, 389–396.

- (30) Ray, S. S.; Maiti, P.; Okamoto, M.; Yamada, K.; Ueda, K. *Macromolecules* **2002**, *35*, 3104–3110.
 (31) Maiti, P.; Yamada, K.; Okamoto, M.; Ueda, K.; Okamoto, K. *Chem. Mater.* **2002**, *14*, 4654–4661.
 (32) Pluta, M.; Galeski, A.; Alexandre, M.; Paul, M. A.; Dubois, P. *J. Appl. Polym. Sci.* **2002**, *86*, 1497–1506.

Table 1. Characteristics of Organoclays^a

Clay Type	Extent of Modification [meq/100g clay]	Chemical Structure of Organic Modifier
Cloisite 30B	90	
Cloisite 25A	95	
Cloisite 15A	125	

^aHT is hydrogenated tallow (~65% C18; ~30% C16; ~5% C14).

composite compositions were based on the inorganic component of the modified clay thereby excluding the amount of organic modifier. (The inorganic amount in each of the organoclays was obtained by analysis of 10 mg of modified clay via thermal gravimetric analysis under dried air flow at 900 °C.) Both the PLLA solution and clay suspension were sonicated separately for 30 min with a Misonix 3000 probe sonicator at 21 W and room temperature (pulse mode was used to prevent an extensive increase in temperature) and subsequently mixed. The final mixture was further sonicated for 30 min. The mixture was then cast on a glass surface and kept in a desiccator for controlled evaporation of the solvent over 2 d. Eventually optically clear nanocomposite films with thickness ranging from 500 to 700 μm were obtained and subsequently dried at 80 °C under vacuum for 2 d. A list of prepared samples is shown in Table 2.

Characterization. *X-ray Diffraction.* XRD experiments were performed in transmission mode on a pinhole-collimated camera equipped with a Rigaku copper target rotating anode (Cu Kα radiation $\lambda = 1.54 \text{ \AA}$) operated at 3.6 kW (36 kV and 100 mA). Data were collected with a Bruker 2-dimensional detector at 4- and 120-cm camera lengths. The isotropically scattered data were azimuthally integrated into one-dimensional profiles of intensity versus scattering angle, 2θ , and normalized with respect to relative intensity of the peaks. The samples were scanned several times and rotated/translated between scans to ensure no orientation existed in the samples and, correspondingly, isotropic scattering resulted in all samples.

Transmission Electron Microscopy. TEM bright field imaging was performed with a JEOL 2000FX microscope using 200 kV accelerating voltage. Samples were embedded in epoxy resin (Araldite 502, dodecyl succinic anhydride (DDSA), DMP 30), cured at 60 °C overnight, and subsequently microtomed at room temperature into ultrathin slices (<100-nm thickness) using a Diatome diamond knife. Sections were collected with 300-mesh carbon coated copper grids and were observed without any further modification or coating.

Thermal Analysis. To precisely observe the effect of clay incorporation on PLLA crystallinity DSC experiments were performed with a TA-Instruments DSC model Q100 series instrument under constant nitrogen flow with a heating rate of 10 °C/min. The DSC samples were weighed such that all of the samples had identical PLLA content. The sample weight was maintained at low levels (1–2 mg) for all measurements to minimize any possible thermal lag during the scans. Each reported result is an average of four different measurements. Temperature and heat of fusion were calibrated with an Indium standard and background subtraction was done according to TA instruments protocols.

Mechanical Analysis. DMA experiments were performed on a TA instruments 2980 DMA apparatus equipped with a film tension clamp. The instrument was programmed to measure E' (storage modulus) over the range of 30–150 °C at 2 °C/min heating rate and 1 Hz constant frequency. Calibrations for

force, mass, position, and temperature were made in accordance with TA procedures. The specimen films were cut with length-to-width ratios >6 to guarantee uniform strain in the films under tension. The applied strain (0.02–0.05%) was well within the linear viscoelastic region of the samples and the collected data were reproducible.

Results and Discussion

Morphology. Morphology of PLSNs is typically probed by XRD and TEM techniques. X-ray diffraction studies provide a quantitative understanding of the global morphology in reciprocal space, whereas TEM quantitatively visualizes the complimentary local structure in real space. X-ray diffraction patterns of neat PLLA, neat organoclays, and 2, 5, 10, and 15 wt % clay in PLLA nanocomposites are shown in Figures 2–4(a). The pure organoclay diffraction intensities were divided by a factor of 100 relative to the nanocomposite intensities in order to place them on the same plots for comparison. The nanocomposite diffraction intensities were vertically offset for clarity of presentation. The diffraction corresponding to the crystalline regions of pure PLLA has several characteristic peaks, the two strongest of which are labeled C and D in each of the figures. The crystal structure of PLLA has been the topic of extensive studies.^{33–35} PLLA has two crystal structures: a pseudoorthorhombic α structure with left-handed 10/3 helices chain conformation and a less stable orthorhombic β structure with 3/1 chain conformation.³⁵ The PLLA diffraction patterns presented herein most closely match the α crystalline structure. In all of the nanocomposites, because the positions of the peaks corresponding to the crystal structure of the PLLA are not altered, lattice parameters were not altered by altering the amount of clay incorporation. These peaks are present in all the nanocomposite XRD patterns indicating that the organoclay has not significantly disrupted crystallization or altered the crystal structure within the PLLA matrix. However, by incorporation of organoclay, regardless of the modifier, intensity of these peaks did slightly diminish, indicative of a decrease in the amount of crystallinity due to organoclay platelets. This decrease in crystallinity of the matrix is in accordance with the observed decrease in heat of fusion as measured by DSC and shown in Figure 5a–c (vide infra). A detailed study of the effect of organoclay on crystallization behavior of PLLA, which is beyond the scope of this contribution, will be presented elsewhere.³⁶

According to Figure 2(a) the characteristic peak of neat Cloisite 15A that corresponds to the interlayer spacing, $d(001) = 32.36 \text{ \AA}$ (B), is shifted to 38.08 Å (A) due to the intercalation of matrix PLLA into the clay galleries. The intensity of this intercalated clay peak (A) gradually increases with addition of the organoclay. This increase in intensity is simply due to more diffracted X-rays from the parallel assembly of the additional intercalated clay.

In the case of Cloisite 25A-based nanocomposites, Figure 3(a), the characteristic peak of pristine organo-

(33) Desantis, P.; Kovacs, A. J. *Biopolymers* **1968**, *6*, 299.

(34) Brizzolara, D.; Cantow, H. J.; Diederichs, K.; Keller, E.; Domb, A. J. *Macromolecules* **1996**, *29*, 191–197.

(35) Hoogsteen, W.; Postema, A. R.; Pennings, A. J.; Tenbrinke, G.; Zugenmaier, P. *Macromolecules* **1990**, *23*, 634–642.

(36) Krikorian, V.; Schultz, J. M.; Pochan, D. J. *Macromolecules*. To be submitted for publication.

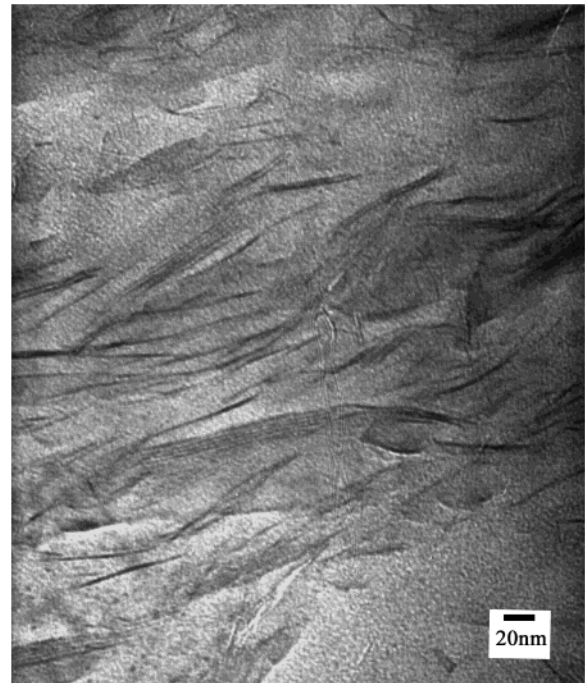
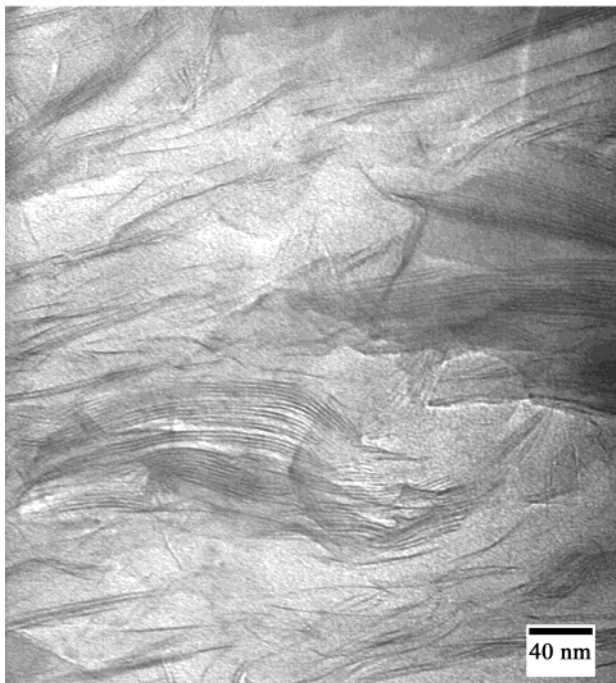
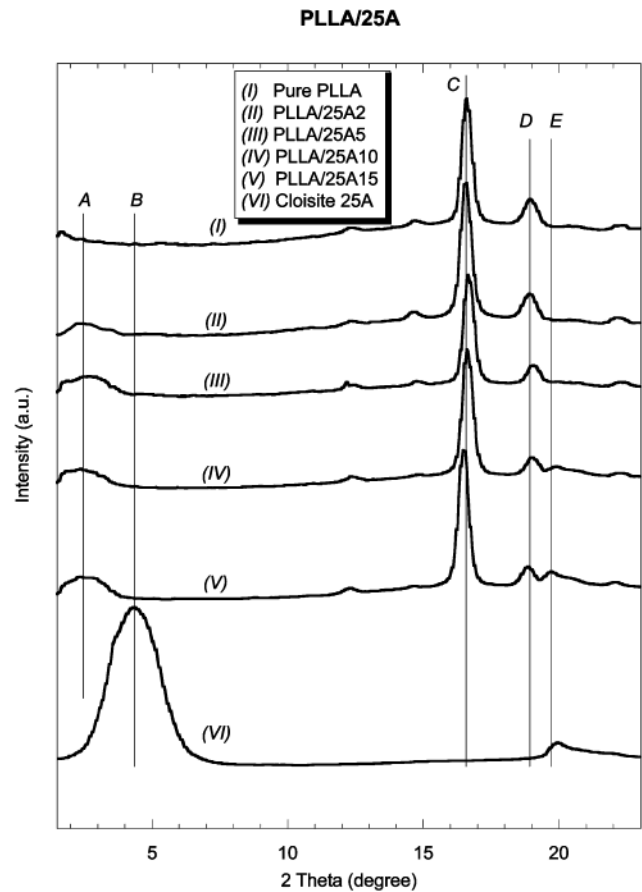
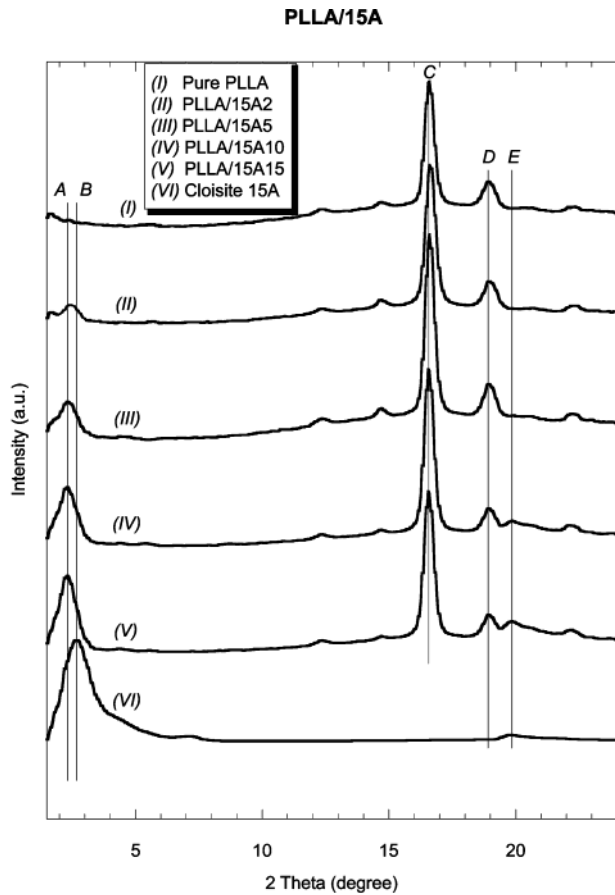


Figure 2. (a). Comparison of XRD patterns for different compositions of neat PLLA, 2, 5, 10, and 15 wt % Cloisite 15A in PLLA nanocomposites, and neat Cloisite 15A. (A) The first-order reflection originating from the interplatelet long spacing after PLLA intercalation, which corresponds to 38.08 Å. (B) The first-order reflection $d(001)$ originating from the interplatelet long spacing of pure Cloisite 15A, which corresponds to 32.36 Å spacing. (C) and (D) Strong diffraction peaks of crystalline regions of neat PLLA corresponding to spacings of 5.34 and 4.67 Å, respectively. (b). Bright field transmission electron micrograph of the sample with 10 wt % Cloisite 15A.

Figure 3. (a). Comparison of XRD patterns for different compositions of neat PLLA, 2, 5, 10, and 15 wt % Cloisite 25A in PLLA nanocomposites, and neat Cloisite 25A. (A) First-order reflection originating from the interplatelet long spacing after PLLA intercalation, which corresponds to 36.03 Å. (B) First-order reflection $d(001)$ originating from the interplatelet long spacing of pure Cloisite 25A, which corresponds to 20.04 Å spacing. (C) and (D) Strong diffraction peaks of crystalline regions of neat PLLA corresponding to spacings of 5.34 and 4.67 Å, respectively. (b). Bright field transmission electron micrograph of the sample with 10 wt % Cloisite 25A.

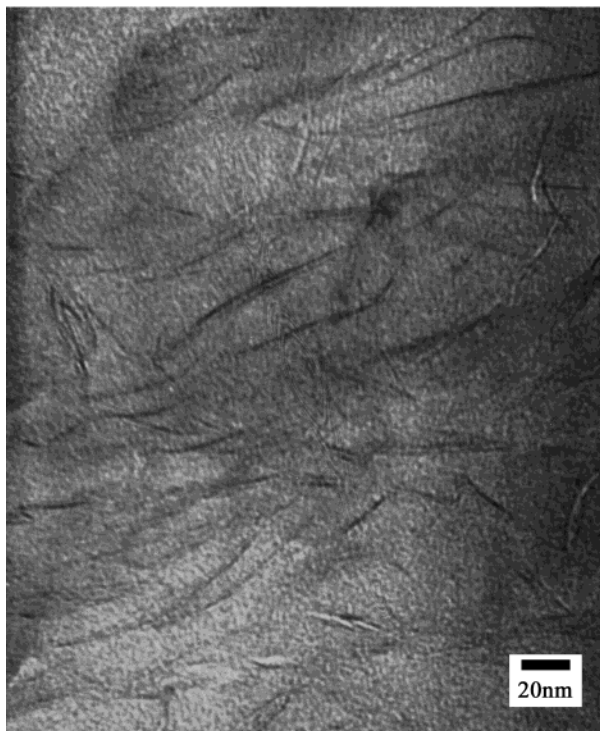
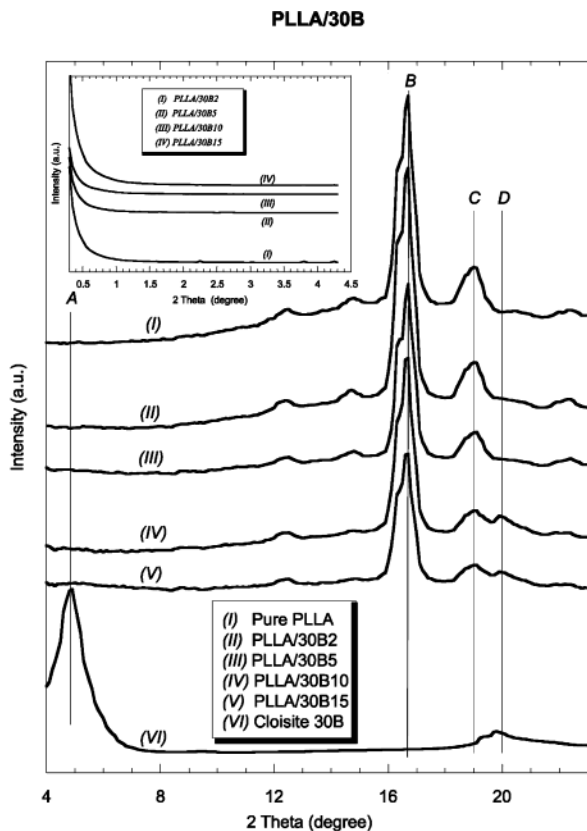


Figure 4. (a). Comparison of XRD patterns for different compositions of neat PLLA, 2, 5, 10, and 15 wt % Cloisite 30B in PLLA nanocomposites, and neat Cloisite 30B. (A) First-order reflection $d(001)$ originating from the interplatelet long spacing of pure Cloisite 30B, which corresponds to 18.26 Å spacing. (B) and (C) Strong diffraction peaks of crystalline regions of neat PLLA corresponding to spacings of 5.34 and 4.67 Å, respectively. (Inset) Small-angle X-ray scattering diffractograms for different Cloisite 30B loadings. (b). Bright field transmission electron micrograph of the sample with 10 wt % Cloisite 30B.

Table 2. Characteristics of Samples Prepared (Designation, Clay Type, and Clay Content)

sample	type of clay	clay content (inorganic part) (wt %)
PLLA/15A2	15A	2
PLLA/15A5	15A	5
PLLA/15A10	15A	10
PLLA/15A15	15A	15
PLLA/25A2	25A	2
PLLA/25A5	25A	5
PLLA/25A10	25A	10
PLLA/25A15	25A	15
PLLA/30B2	30B	2
PLLA/30B5	30B	5
PLLA/30B10	30B	10
PLLA/30B15	30B	15

Table 3. Solubility Parameters Calculated by Group Contribution Methods

	Fedors	Van Krevelen	Hoy	Small	Hoftyzer & Van Krevelen
PLLA	22.75	21.23	22.72	22.36	21.56
30B	21.44	19.49	18.73		
25A	17.23	16.45	15.65		
15A	18.13	16.91	16.74		

clay, $d(001) = 20.04$ Å (B), is shifted to higher d spacings, 36.03 Å (A) and broadened. The interlayer spacing is significantly larger relative to that of Cloisite 15A and is observed across all nanocomposite compositions. The broadening of the peak is due to partial disruption of parallel stacking or layer registry of the pristine organoclay, which reveals the existence of some exfoliated clay platelets. Therefore, a mixture of exfoliated and intercalated structure is observed at all different Cloisite 25A clay loadings. This intercalation/exfoliation coexistence is in agreement with the TEM data in Figure 3(b).

In the final case of Cloisite 30B, Figure 4(a), there is no evidence of an organoclay basal spacing peak, 18.26 Å (A) in the pure organoclay, across all nanocomposite compositions. Small-angle X-ray scattering data (inset of Figure 4(a)) also do not show any ordered structure at low angles/large d spacings. This lack of intergallery clay diffraction is due to the complete exfoliation and random distribution of the clay platelets within the PLLA matrix and is supported by TEM data (Figure 4(b)). This fully exfoliated morphology is stable; the silicate layers do not re-aggregate and form intercalated tactoids after melting and recrystallizing of the PLLA matrix.³⁶

TEM analysis can be used to support XRD results by visualizing clay dispersion on the nanoscale. Typical TEM micrographs of the 10 wt-% nanocomposites with different clay modifiers are shown in Figures 2–4(b). Nanometer-range intercalated clay tactoids are clearly shown in Figure 2(b). Dark lines correspond to the cross section of a clay sheet ca. 1 nm thick and the gap between two adjacent lines is the interlayer spacing or gallery. The measured interlayer spacings between adjacent clay layers of intercalated tactoids obtained from TEM are consistent with the XRD data. Figure 3(b), a composite of PLLA and Cloisite 25A, reveals a coexistence of disordered, exfoliated platelets of clay layers and intercalated tactoids. Fully exfoliated clay structure can be seen in Figure 4(b), which corresponds to the PLLA/30B10 sample. Extensive TEM observa-

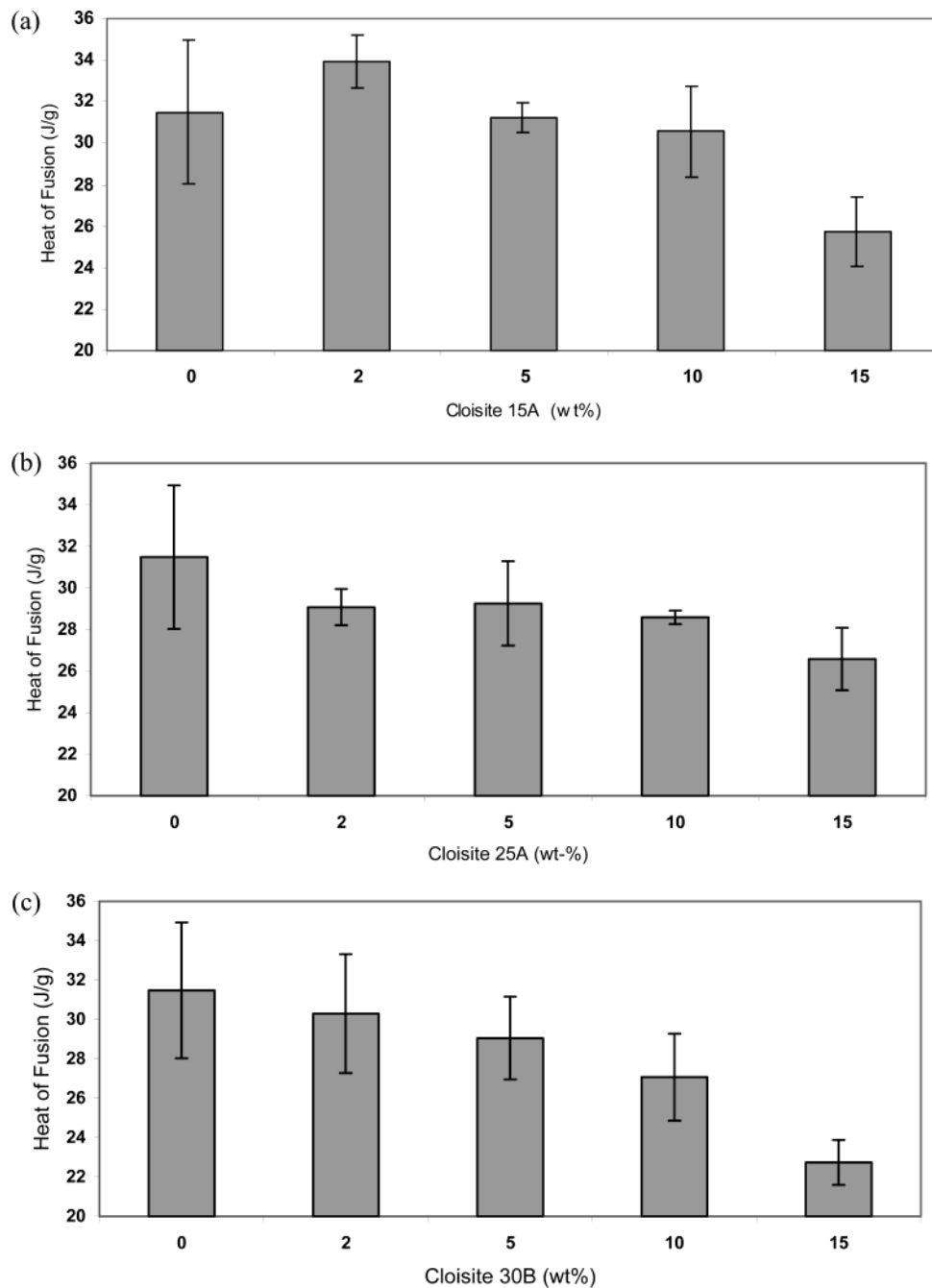


Figure 5. Heat of fusion variations of PLLA nanocomposites with respect to clay composition: (a) Cloisite 15A, (b) Cloisite 25A, and (c) Cloisite 30B. Results of three measurements are shown with the data point representing the middle observed value and the error bars representing the total spread of the three measurements.

tions reveal the homogeneous dispersion of clay platelets in nanometer range throughout the PLLA/30B10 sample without aggregation or tactoid formation.

Enthalpic interactions between the matrix polymer and organic clay modifier play an important role in the extent of organoclay dispersion. A high degree of miscibility between modifier and matrix will provide a larger driving force for silicate platelet exfoliation and stacked clay structure disruption. As a rough estimation of degree of miscibility of the neat PLLA in different organoclays we have calculated the solubility parameters (δ) for each of the organic modifiers used in the organoclays (Table 1) and neat PLLA by using group contribution methods of Fedors, Van Krevelen, Hoy, Small, and Hoftyzer–Van Krevelen,³⁷ Table 3. Please

refer to the Supporting Information for more description of these methods. The solubility parameters calculated for pure PLLA are closest to those of the modifier used in Cloisite 30B, which suggests the best miscibility/highest compatibility of the 30B filler with the PLLA matrix. This is in accordance with the fully exfoliated morphology observed in the previously discussed WAXS and TEM experiments.

Despite the higher extent of modification in Cloisite 15A, and its larger basal d spacing as compared to that of Cloisite 25A and Cloisite 30B, a lower degree of exfoliation is obtained. This suggests that the key factor

(37) Krevelen, D. W. V. *Properties of Polymers*; Elsevier: Amsterdam, The Netherlands, 1990.

for complete exfoliation of the silicate layers throughout the PLLA matrix is the degree of miscibility of the organic modifier and the PLLA. Interaction of C=O bonds on the backbone of PLLA with the diols present in the Cloisite 30B organic modifier seem to play a key role in thorough dispersion of silicate layers in PLLA and compensates for the smaller interlayer gallery spacing and lower extent of modification. To the best of our knowledge this system is the first fully exfoliated PLLA based nanocomposite and all the previous works ended up with intercalated^{30,31,38,39} or phase-separated²⁹ composites. The degree of clay dispersion in the matrix plays a key role in the degree of enhancement of the matrix properties. Nanometer-range dispersion of the clay platelets in polymer matrix, i.e., higher amount of exfoliation, gives rise to better barrier properties²⁰ because it increases the mean free path of the gas molecules. Also, higher mechanical properties are expected because of the higher surface interaction in exfoliated nanocomposites relative to intercalated systems.

Thermal Characterization. DSC experiments were carried out on three different samples of each nanocomposite composition. By integrating the area under the endothermic region of the DSC curves, the heat of fusion for each of the nanocomposite compositions was calculated. Variation of heat of fusion between samples with different clay compositions relative to pure PLLA is shown in Figure 5a–c. Generally, the highest heat of fusion (i.e., highest percent of crystallinity) was observed in pure PLLA. Increasing the clay content, regardless of its organic modification type, reduces the heat of fusion, which indicates the percent of crystallinity is decreased by inorganic phase incorporation. This effect is most obvious in the case of Cloisite 30B-based nanocomposites (Figure 5c) in which, according to XRD and TEM data, the aluminosilicate layers are fully dispersed within the matrix. This full dispersion can be related to the favorable interaction of the organophilic modified clay platelets with the polymer backbone, which consequently hinders the mobility and flexibility of the polymer to fold and join the crystallization growth front. Decrease in amount of crystallinity is also indicated by the decrease in intensity of the diffraction peaks corresponding to the crystalline lamellae of the polymer, Figures 2–4(a).

Melting points (T_m) of the samples were evaluated from the position of the maximum in the endothermic peaks of DSC thermographs. The melting point of all of the nanocomposites was 177.05 ± 0.3 °C. This indicates clay loading does not significantly alter the melting point of the PLLA. The crystalline lamellar thickness did not change and only the percentage of crystalline regions throughout the samples decreased with increased clay content.

Mechanical Properties. Figure 6 shows the temperature dependence of the storage tensile modulus, E' , of the neat PLLA and PLLA with different clay loadings over the range of 20–150 °C. Each of the curves represents at least five different measurements provid-

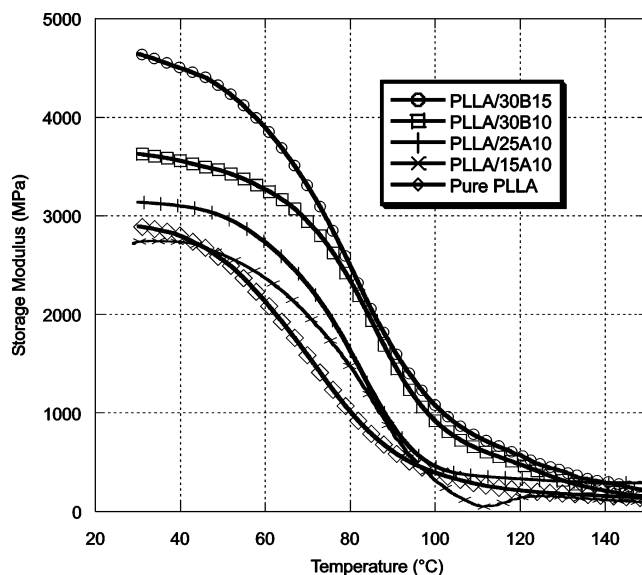


Figure 6. Dynamic viscoelastic behavior of neat PLLA, PLLA/30B10, PLLA/15A10, PLLA/25A10, and PLLA/30B15.

ing a standard deviation $< \pm 200$ MPa. An apparent glass transition is revealed by a steep decrease of storage modulus followed by the initial glassy plateau in all of the samples. This temperature is not significantly affected by clay incorporation. Over the entire temperature range, the storage modulus of the 15 wt % organoclay content sample is higher than that of 10 wt % and neat PLLA. Around body temperature for 15 and 10 wt % loadings are 61.4% and 26.4%, respectively, compared to neat PLLA. On the other hand, at higher temperatures, above 120 °C, all the samples reach a plateau, which suggests a rubberlike structure composed of both crystalline and amorphous phases. In plateau regions above 120 °C, the storage modulus difference between neat PLLA and the reinforced samples tends to zero. This phenomenon is also observed in poly (*L*-lysine)/Na⁺-MMT systems in which, after a specific temperature, the effect of clay on the storage modulus becomes negligible and the nanocomposite stiffness becomes matrix dependent.²¹ Comparing the three different modified clay nanocomposite samples with 10 wt % clay loading reveals that in the case of fully exfoliated system, 30B, a higher storage modulus is achieved due to the larger surface area between reinforcement phase and polymer matrix.

Conclusion

We have explored the effect of compatibility of different organic modifiers on the overall extent of dispersion of aluminosilicate layers in a PLLA matrix. Three different commercially available organoclays were used as a reinforcement phase. Nanocomposites were fabricated via the exfoliation adsorption technique by dispersion of organoclay in a suitable solvent and subsequent mixing with PLLA. According to TEM and XRD studies an increase in miscibility of the organic modifier with the PLLA matrix increased the tendency of the aluminosilicate layers to exfoliate. In the case of Cloisite 30B organoclay the favorable enthalpic interaction between diols present in the organic modifier with the C=O bonds present in the PLLA backbone is a significant

(38) Ray, S. S.; Yamada, K.; Okamoto, M.; Ueda, K. *Nano Lett.* **2002**, *2*, 1093–1096.

(39) Ray, S. S.; Okamoto, K.; Yamada, K.; Okamoto, M. *Nano Lett.* **2002**, *2*, 423–425.

factor for driving the system toward exfoliation. This is the primary factor that was not present in organoclays used in previous investigations^{29–31,40} that resulted in primarily microphase separation or intercalation of the PLLA. According to the DSC measurements crystallinity of the PLLA is suppressed because of the addition of organoclay, with the most significant suppression observed with complete clay exfoliation. Addition of organoclays did not alter the melting point of PLLA, which suggests intact crystalline lamellae thickness, in accordance with corresponding XRD crystalline peaks of PLLA. Mechanical properties of the nanocomposites show significant improvements compared to neat PLLA due to the nanometer range dispersion of the clay

platelets. Higher clay incorporation and a higher degree of exfoliation gave rise to stiffer materials with optically transparent properties.

Acknowledgment. We are grateful to the Center of Composite Materials (CCM) at UD for use of DMA and the College of Engineering Keck Electron Microscopy Laboratory.

Supporting Information Available: Group contribution methods of Fedors, Van Krevelen, Hoy, Small, and Hoftyzer–Van Krevelen for calculation of solubility parameters, and a representative calculation of solubility parameters for neat PLLA (Table 4). This material is available free of charge via the Internet at <http://pubs.acs.org>.

(40) Ray, S. S.; Yamada, K.; Okamoto, M.; Ogami, A.; Ueda, K. *Chem. Mater.* **2003**, *15*, 1456–1465.

CM034369+